

Short-video Propagation Influence Rating: A New Real-world Dataset and A New Large Graph Model

Dizhan Xue, Shengsheng Qian, Chuanrui Hu, Changsheng Xu, *Fellow, IEEE*

Abstract—Short-video platforms have gained immense popularity, captivating the interest of millions, if not billions, of users globally. Recently, researchers have highlighted the significance of analyzing the propagation of short-videos, which typically involves discovering commercial values, public opinions, user behaviors, etc. This paper proposes a new Short-video Propagation Influence Rating (SPIR) task and aims to promote SPIR from both the dataset and method perspectives. First, we propose a new Cross-platform Short-Video (XS-Video) dataset, which aims to provide a large-scale and real-world short-video propagation network across various platforms to facilitate the research on short-video propagation. Our XS-Video dataset includes 117,720 videos, 381,926 samples, and 535 topics across 5 biggest Chinese platforms, annotated with the propagation influence from level 0 to 9. To the best of our knowledge, this is the first large-scale short-video dataset that contains cross-platform data or provides all of the views, likes, shares, collects, fans, comments, and comment content. Second, we propose a Large Graph Model (LGM) named NetGPT, based on a novel three-stage training mechanism, to bridge heterogeneous graph-structured data with the powerful reasoning ability and knowledge of Large Language Models (LLMs). Our NetGPT can comprehend and analyze the short-video propagation graph, enabling it to predict the long-term propagation influence of short-videos. Comprehensive experimental results evaluated by both classification and regression metrics on our XS-Video dataset indicate the superiority of our method for SPIR. Our dataset and code will be open upon acceptance.

Index Terms—Short-video propagation, dataset, large graph model



1 INTRODUCTION

SHORT-VIDEO platforms, such as Tiktok (aka Douyin)¹, Kwai (aka Kuaishou)², and Xigua³, have gained immense popularity, captivating the interest of millions, if not billions, of users globally. The users are capable of publishing their activities, opinions, and thoughts by posting, commenting, and sharing various forms of online content, including text, images, and videos. Consequently, these overwhelming user behaviors and user-generated content have formed a huge and intricate propagation network, harboring a wealth of information about our society. Recently, researchers have highlighted the significance of analyzing the propagation of short-videos [1]–[3], which typically involves discovering commercial values, public opinions, user behaviors, etc. Traditional research mainly focuses on forecasting the popularity of videos [4]–[6] measured by a single indicator, such as the number of views or likes. However,

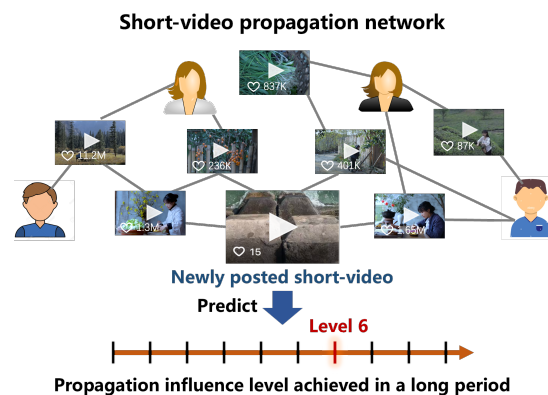


Fig. 1. Short-video Propagation Influence Rating (SPIR): Predicting the influence level of a newly posted short-video that can be achieved in a long period.

real-world propagation behaviors are more complex and can include sharing, collecting, commenting, etc.

To address the above limitation, we attempt to evaluate the propagation influence by simultaneously considering as many interactive indicators as possible, including views, likes, shares, collects, comments, etc. Moreover, as shown in Figure 1, we propose a new task named *Short-video Propagation Influence Rating* (SPIR), which aims to predict the long-term propagation influence of a newly posted short-video, under the background of a huge propagation network. Different from traditional popularity prediction that forecasts a single interactive indicator over a short period (e.g., several hours [1], [6]), our SPIR predicts the comprehensive

Manuscript received MM DD, YY; revised MM DD, YY. (Corresponding author: Shengsheng Qian.)

- Dizhan Xue, Shengsheng Qian, and Changsheng Xu are with State Key Laboratory of Multimodal Artificial Intelligence Systems, Institute of Automation, Chinese Academy of Sciences, Beijing 100190, China, and also with School of Artificial Intelligence, University of Chinese Academy of Sciences (e-mail: xuedizhan17@mailsucas.ac.cn; shengsheng.qian@nlpr.ia.ac.cn; csxu@nlpr.ia.ac.cn)
- Chuanrui Hu is with Qihoo 360 AI lab, Beijing 100026, China (e-mail: huchuanrui_1206@163.com).

1. <https://www.tiktok.com/>

2. <https://www.kwai.com/>

3. <https://www.ixigua.com/>

TABLE 1

A brief comparison of information collected in different short-video propagation datasets. ✓ means provided and ✗ means unprovided.

Dataset	#Platforms	Views	Likes	Shares	Collects	Fans	Comments	Comment Content	#Videos	#Samples	#Users
Daum [7]	1	✓	✗	✗	✗	✗	✗	✗	196,037	196,037	Unknown
Youtube [8]	1	✓	✓	✗	✗	✓	✓	✗	1,761	1,761	Unknown
NUS [4]	1	✓	✓	✗	✗	✓	✓	✗	303,242	303,242	98,166
Xigua [5]	1	✓	✗	✗	✗	✗	✗	✗	11,219	11,219	2,664
MicroLens [2]	1	✓	✓	✗	✗	✗	✗	✗	19,738	19,738	100,000
XS-Video (Ours)	5	✓	✓	✓	✓	✓	✓	✓	117,720	381,926	419,374

propagation influence assessed through multi-dimensional interactions accumulated over a long period. SPIR requires a model to thoroughly analyze the multimodal content features, interactive information, and propagation relationships within a short-video. Subsequently, a rating from 0 to 9 is assigned to represent the propagation influence of this video that can be achieved over a long period. The development of SPIR systems can potentially benefit a wide spectrum of real-world applications on short-video platforms, including advertising [9], [10], recommendation [11], [12], and democracy [13], [14]. In this paper, we attempt to promote the research of SPIR from both the data and model perspectives, proposing the first cross-modal short-video propagation dataset and a novel large graph model for SPIR.

To promote the research of SPIR and short-video propagation analysis, we propose a large-scale Cross-platform Short-Video (XS-Video) dataset, where videos are collected from the 5 biggest Chinese platforms (i.e., Douyin, Kuaishou, Xigua, Toutiao, and Bilibili). Though hot topics and content are typically discussed and replicated across platforms, almost all existing datasets collect data from a single platform and lack a broad scope of short-videos. As compared in Table 1, our XS-Video dataset significantly surpasses the existing datasets in terms of platform numbers and interactive indicator coverage, while also containing comment content and more samples and users. Specifically, we collect 381,926 states/samples of 117,720 short-videos within several days after their publication, belonging to 535 topics. Different states/samples of the same video are distinguished by their sampling times, as well as the interactions and comment content at those times. Furthermore, we annotate the propagation influence level of all short-videos according to their multi-dimensional interactive indicators over a two-week period following their publication, since almost all short-videos peak in interactions within two weeks. We demonstrate a short-video sample in the XS-Video dataset in Figure 2. Moreover, utilizing the entities and relations present in XS-Video, we construct a huge propagation graph consisting of 5.5 million nodes of videos, topics, comments, various interactions, etc., and 1.7 billion directed edges between these nodes. More details about our dataset and the constructed propagation graph are provided in Section 3.6. Compared to existing datasets, XS-Video provides more comprehensive information on video content, post, interactions, and comments, which is essential for the research on short-video propagation, including our SPIR task.

We build a comprehensive benchmark for SPIR by evaluating state-of-the-art methods, including Graph Neural

Fig. 2. An example of short-video states/samples collected in our XS-Video dataset. The text is translated into English.

Networks (GNNs), Large Language Models (LLMs), and multimodal LLMs. Surprisingly, these state-of-the-art methods are far from satisfactory for short-video propagation analysis. To improve the accuracy of SPIR and leverage the advancements in LLMs, we propose a Large Graph Model (LGM) named NetGPT. Our model can capture both the propagation network structure and heterogenous short-video features while utilizing the pretraining knowledge to predict the propagation influence level. LLMs have recently shown powerful reasoning ability for text, images, and even videos [15]–[19]. Current research has explored adapting LLMs for analyzing textual graph data [20]–[22]. However, bridging heterogeneous graph data and LLMs is still an open problem, especially as we cannot input our huge propagation graph into an LLM. Our experiments also reveal that LLMs cannot directly learn the graph-structured relations in short-video propagation data, which results in poor performance for SPIR. To address this limitation, we propose a three-stage training mechanism for establishing an effective LGM, including Heterogeneous Graph Pretraining, Supervised Language Fine-tuning, and Task-oriented Predictor Fine-tuning. Finally, we can empower LLMs (e.g., Qwen2-VL [18] in our experiments) to comprehend and analyze the short-video propagation graph. Our NetGPT model significantly outperforms state-of-the-art baselines, including Graph Neural Networks (GNNs), LLMs, and multimodal LLMs on our XS-Video dataset.

In brief, the contributions of our work are as follows:

- We propose the Short-video Propagation Influence Rating (SPIR) task, which aims to predict the long-term propagation influence of a newly posted short-video in a huge propagation network. Different from traditional popularity prediction that forecasts a single interactive indicator over a short period (e.g., several hours [1], [6]),

SPIR predicts the comprehensive propagation influence assessed through multi-dimensional interactions over a long period.

- We propose XS-Video, a large-scale real-world dataset for short-video propagation comprising 381,926 samples with comprehensive content and interactive information collected from the 5 biggest Chinese platforms. Moreover, utilizing the entities and relations present in XS-Video, we construct a huge propagation graph consisting of 5.5 million nodes and 1.7 billion directed edges.
- We build a comprehensive benchmark for SPIR by evaluating state-of-the-art methods, including GNNs, LLMs, and multimodal LLMs. Surprisingly, these methods are far from satisfactory. These results motivate us to propose NetGPT, a novel Large Graph Model (LGM) that can bridge heterogeneous graph data and LLMs, based on a novel three-stage training mechanism. Experiments on XS-Video indicate that NetGPT significantly outperforms the state-of-the-art methods.

2 RELATED WORK

2.1 Short-Video Propagation Influence Analysis

Existing research on short-video propagation influence analysis mainly focuses on the popularity prediction of short-videos, such as predicting the views of newly posted videos [23]–[27]. For example, Chen et al. [4] focus on the short-video representation and present a transductive multimodal learning model for short-video popularity prediction. Xie et al. [5] propose a multimodal variational encoder-decoder framework that considers the uncertain factors as the randomness for the mapping from the multimodal features to the popularity. Xie et al. [6] propose a hierarchical multimodal variational encoder-decoder to predict the popularity of short-videos by comprehensively leveraging user information and the short-video content in a hierarchical fashion. Zhou et al. [2] present a multimodal retrieval-augmented popularity prediction model that improves prediction accuracy using relevant retrieved information.

However, the above research primarily focuses on forecasting some interactive indicators on a single platform, such as views or likes. While these indicators can provide a perspective into the popularity of videos, they fail to offer a comprehensive evaluation of video influence. In reality, the propagation behaviors are far more complex and multifaceted. Users engage in various actions that contribute to the cross-platform spread and influence of videos, including sharing, collecting, liking, and commenting videos. Therefore, to advance research in short-video propagation analysis, we propose a large-scale real-world XS-Video dataset. XS-Video collects cross-platform videos and offers a more comprehensive array of information, including videos, titles, topics, descriptions, 5 interactive indicators, and comment content, etc. Our dataset aims to facilitate a deeper research on propagation dynamics.

2.2 Large Graph Model

Recent advancements in Large Language Models (LLMs) have showcased their impressive reasoning abilities not

only with text but also with images and videos [28]–[31]. This progress has led to an increasing focus on adapting LLMs for analyzing graph-structured data, especially textual graphs. For instance, Li et al. [21] utilize LLM prompting on textual graphs, offering substantial potential to enhance graph transfer capabilities across diverse tasks and domains. Tang et al. [20] integrate LLMs with graph structural knowledge through graph instruction tuning, which includes a text-graph grounding component, a dual-stage instruction tuning approach, and a graph-text alignment projector. Wang et al. [22] propose Build-a-Graph Prompting and Algorithmic Prompting, two instruction-based approaches to enhance LLMs in solving natural language graph problems.

However, the above work focuses on textual graphs where the information of nodes and edges can be transformed into text, thereby directly leveraging the textual reasoning ability of LLMs. These methods cannot be directly applied to our heterogeneous propagation graph of texts, videos, times, and scalars. Therefore, we propose NetGPT to capture both the propagation network structure and heterogeneous short-video features, while utilizing the pretraining knowledge for SPIR.

3 DATASET

Analyzing propagation patterns on short-video platforms can aid in discovering high-value content, public opinions, and user preferences, thereby creating commercial and social value. Our proposed dataset aims to provide a realistic and large-scale benchmark for the research on short-video propagation. As briefly shown in Table 1 and Figure 2, compared to previous short-video propagation datasets [2], [4], [5], [7], [8], our dataset has three key advantages: (1) While existing datasets separately collect data from a single short-video platform, we collect short-videos from the 5 biggest Chinese platforms, which provide cross-platform propagation information; (2) Instead of focusing on a subset of interactive indicators, we gather a wide range of indicators such as views, likes, shares, collects, fans, and comments, which facilitate deep analysis of video interactions; (3) Our dataset contains more samples and users, while providing more comprehensive short-video content, including videos, titles, descriptions, topics, and the related comment content. Figure 3 demonstrates a brief construction procedure of our dataset.

3.1 Data Collection and Cleaning

Utilizing the keywords of 535 trending topics on the Chinese Internet between November 25th, 2024 and January 2nd, 2025, we crawl site data of relevant short-videos with durations of less than 5 minutes from the 5 biggest Chinese platforms, i.e., Douyin, Kuaishou, Xigua, Toutiao, and Bilibili. Furthermore, we trace the interactive information of all videos until more than two weeks after their post. Since almost all short-videos peak in interactive indicators and lose popularity within two weeks, our collected data is enough for assessing the long-term propagation influence of short-videos (as further analyzed in Appendix 3.4).

Given active topics which include daily and historical trending topics on the Chinese Internet, we search and crawl

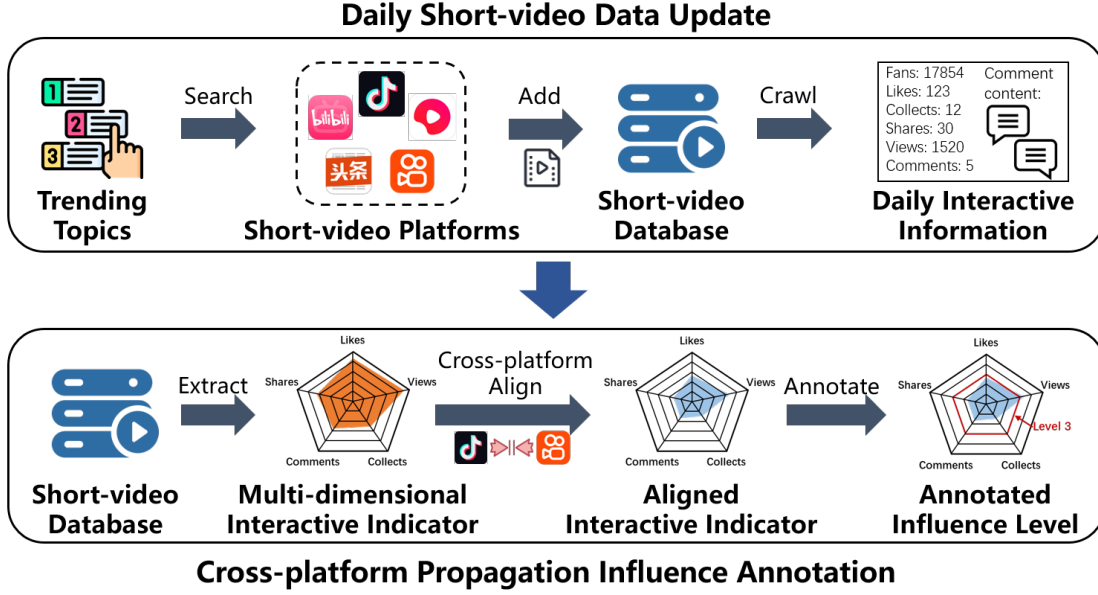


Fig. 3. Brief construction procedure of our XS-Video dataset: (1) Daily update of new short-videos and the interactive information of already collected short-videos; (2) Alignment of multi-dimensional interactive indicators (collected 2 weeks later than the publication of videos) for annotating the video propagation influence levels.

all related short-videos posted in the last 30 days on 5 platforms. However, some trending topics may be similar and correspond to the same concept. Therefore, we conduct a daily data-cleaning procedure by manually merging similar topics, removing low-quality topics, and converting active topics without popularity to inactive topics. For all collected short-videos, we crawl their interactive information every day. Since the interactive information of almost all videos peaks within 2 weeks, if the interactive information 2 weeks later than the post is crawled, we will stop crawling the video. During constructing the data samples, we set the gap of current times of the same short-video as at least 2 days to avoid indistinguishable samples. When constructing the data samples, we ensure that the current time gap between samples belonging to the same short-video is at least two days to prevent indistinguishable samples. The whole data collection procedure is conducted from November 25th, 2024 to January 2nd, 2025. Moreover, we replace user names with anonymous user IDs to avoid privacy problems.

3.2 Cross-platform Propagation Influence Annotation

Cross-platform indicator alignment. To assess the long-term propagation influence of short-videos, we utilize the multi-dimensional interactive indicators accumulated in more than two weeks. However, as the user amounts and activities significantly vary among different platforms (e.g., 0.6 billion daily active users of Douyin versus 0.2 billion monthly active users of Xigua), evaluation through raw interactive indicators cannot effectively annotate the influence of cross-platform short-videos. Therefore, we leverage a novel cross-platform indicator alignment method. First, we additionally collect the short-videos posted by the 199 most popular influencers, covering 27 diverse domains such as social affairs, entertainment, dramas, shopping, celebrity, physical fitness, movie, gaming, relationship, beauty, technology, etc. Since the same short-video posted by the

TABLE 2
Criteria for Propagation Influence Level Annotation.

	Views	Likes	Shares	Collects	Comments
Level 0	0	0	0	0	0
Level 1	>0	>0	>0	>0	>0
Level 2	>100	>10	>10	>10	>10
Level 3	>100000	>20	>20	>20	>20
Level 4	>1000000	>80	>80	>80	>80
Level 5	>1000000	>300	>300	>300	>300
Level 6	>1000000	>1000	>1000	>1000	>1000
Level 7	>10000000	>3000	>3000	>3000	>3000
Level 8	>100000000	>10000	>10000	>10000	>10000
Level 9	>200000000	>50000	>50000	>50000	>50000

same influencer on different platforms should roughly have a similar influence on these platforms, we compute the scaling factor α_* to minimize the Mean Squared Percentage Error (MSPE) of interactive indicators, where $* \in \{\text{Douyin}, \text{Xigua}, \text{Toutiao}, \text{Bilibili}\}$, for the platform $*$ as follows:

$$\alpha_* = \arg \min_{\alpha_*} \frac{1}{|S_*|} \sum_{s \in S_*} \left(\frac{Ind_{Kuaishou}(s) - \alpha_* \cdot Ind_*(s)}{Ind_{Kuaishou}(s) + 1} \right)^2, \quad (1)$$

where S_* are all short-videos posted on both Kuaishou and the platform $*$, and $Ind_*(s)$ is the interactive indicator (i.e., view, like, share, collect, or comments) of the short-video s on the platform $*$. Here, we choose Kuaishou as the central platform since it is the most popular among platforms that provide all 5 interactive indicators.

Finally, we design a stepped classification criteria to rate all short-videos in XS-Video into influence levels 0 to 9, using the aligned multi-dimensional indicators $\alpha_* \cdot Ind_*(v)$. The criteria are designed to make sure that the influence levels follow a natural distribution [32]–[34]. The details of our classification criteria are explained in Appendix 3.3.

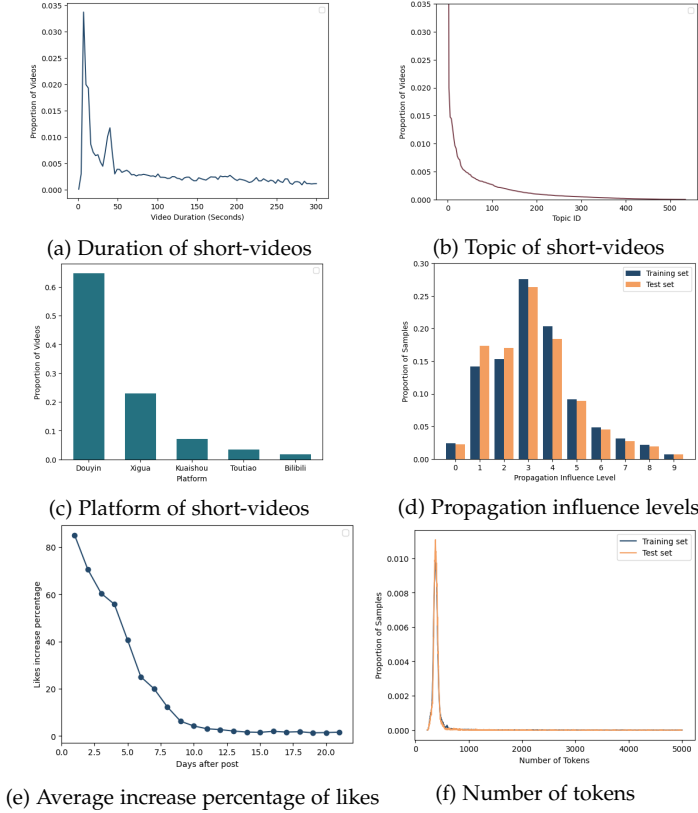


Fig. 4. Distributions of the short-videos and samples in our XS-Video dataset.

3.3 Criteria for Propagation Influence Level Annotation

To evaluate the propagation influence of short videos, our research adopts the cross-platform metrics alignment method described in 3.2 to systematically align the multi-dimensional interaction metrics accumulated over a two-week period. As shown in Table 2, the criteria for dividing the propagation influence level are as follows: when all interactive indicators of a short-video are 0, its influence level is defined as level 0; for the division of the influence level from 1 to 9, a short video is determined to belong to this influence level when its interactive indicator on any of the five dimensions are more than the corresponding level thresholds. The criteria are designed to make sure that the influence levels follow a natural distribution [32]–[34], as shown in Figure 4(d).

3.4 Data Analysis

Our XS-Video dataset consists of 117,720 short-videos, with 304,362 training samples, and 77,564 test samples. The division between the training and test sets is determined by the post date cutoff of December 20th, 2024. All training samples are posted on or before December 20th, 2024, while all test samples are posted after this date. The ratio of the training and test data is around 4:1.

Distribution of short-videos. In Figure 4 (a)-(c), we demonstrate the distributions of durations, topics, and platforms of the collected short-videos. We can observe that the collected short-videos exhibit natural long-tail distributions. While we collect videos with durations from 1s to 5min, the most popular durations are around 7s. Interestingly,

38s is also a subpeak. For topics, we order topic IDs by their popularity. We can find that a small number of head topics account for most of the popularity, while a large number of tail topics only have a small amount of heat. For different platforms, such Matthew effect becomes more obvious. While short-videos posted on Douyin, the most popular Chinese short-video platform, are more than half of all videos, smaller platforms occupy a small proportion of short-videos. To sum up, long-tail distributions inherently exist in short-video data, which may increase the difficulty of analyzing short-video propagation.

Distribution of samples. In Figure 4 (d), we demonstrate the distributions of the annotated propagation influence levels in the training and test sets. The influence distributions are unimodal distributions, where level 3 is the peak of both sets. When the influence further increases, the proportion of samples quickly decreases, exhibiting long-tail distributions on this half (\geq level 3). Moreover, since we adopt a practical division method of the training and test sets by a date boundary, the distributions of these two sets are not identical. This slight mismatch of distributions also increases the difficulty of analyzing short-video propagation.

Increase process of interactive information. To analyze the increase process of interactive information, we compute the daily likes increase percentage as follows:

$$LIP(t) = E\left(\frac{Likes(t) - Likes(t-1)}{Likes(t) + 1}\right), \quad (2)$$

where $Likes(t)$ is the likes in the t -th day after the post of the short-video and $LIP(t)$ is the likes increase percentage of the t -th day. In Figure 4(e), we plot the likes increase percentage of the 1-st to 21-th day after the post. We can observe that the number of likes has become stable since the 10-th day. The similar trends can be observed for other interactive indicators. These results verify our observation that the interactive information of almost all videos peaks within 2 weeks. Therefore, we can utilize the interactive information later than 2 weeks after the post to annotate the final influence level achieved over a long period.

Length of sample information. We analyze the length of the sample information in this section. We utilize the tokenizer of Qwen2-VL to tokenize the sample information in the json format and compute the number of tokens. In Figure 4(f), we demonstrate the distribution of token lengths in XS-Video. We can find that most samples have 200-500 tokens, while some samples with a large amount of comments have thousands of tokens. Moreover, the distributions of token numbers in the training and test sets are similar. Therefore, learning out-of-distribution patterns of long samples is a challenge in XS-Video.

3.5 Example of Samples

We exemplify more samples in XS-Video in Figure 5. In Figure 5(a), the short-video has been posted for two days and gained a large amount of interactions. This short-video finally reaches the level-9 influence level in a long period. In Figure 5(b), the short-video has been posted for just 1 day and gained few interactions. However, this short-video will gain more interactions over a long period and finally reach the level-6 influence level. In Figure 5(c), the short-video has

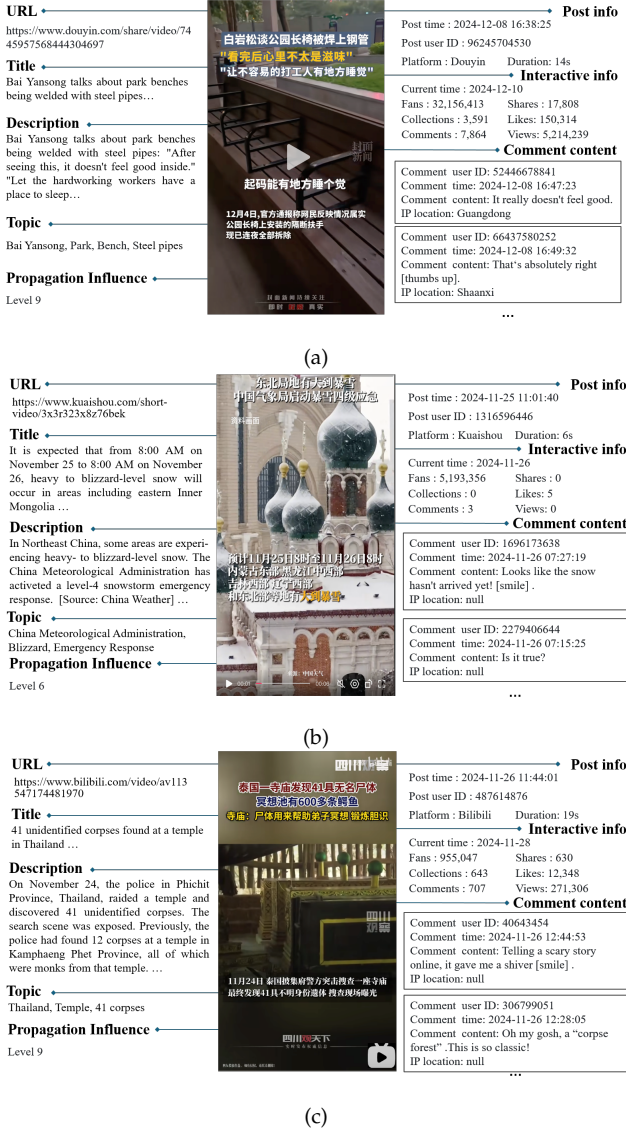


Fig. 5. Examples of samples in our XS-Video dataset.

been posted for two days and gained a lot of interactions. Though the interactions of (c) is much less than those of (a), the user amount of Bilibili is much less than that of Douyin. After the cross-platform interactive information alignment, we annotate that this short-video finally reaches the level-9 influence level on its platform.

3.6 Short-video Propagation Graph

Utilizing the entities and relations present in XS-Video, we construct a huge propagation graph $G = \{V, E, S\}$ with the label set Y . Here V is the vertex set, containing 5 million nodes of videos, platforms, topics, titles, descriptions, comments, various interactive indicators, etc. E is the edge set, containing 1.7 billion directed edges between nodes, which represent the belonging relations between videos and their attributions, common author relations between videos, common topic relations between videos, chronological relations between samples of the same videos, etc. Specially, $S \subset V$ is the set of all video nodes and Y is the set of annotated propagation influence levels of all videos.

Utilizing the entities and relations present in XS-Video, we construct a huge propagation graph consisting of 5.5 million nodes of videos, topics, comments, various interactions, etc., and 1.7 billion directed edges between these nodes. The information about nodes and edges in our graph is shown in Tables 3 and 4, respectively. The short-video propagation graph is a typical heterogenous graph with both heterogenous nodes and edges. In brief, the nodes include the video nodes, the static attribution nodes of videos, and the dynamic interactive nodes of videos. The edges include the edges from the attribution nodes to videos, the interactive nodes to videos, and the video nodes to video nodes.

4 METHOD

Short-video propagation network is typical graph-structured data, where edges (such as video-author and video-video) represent complex propagation relations between entries. State-of-the-art methods for analyzing graph-structured data usually adopt Graph Neural Networks (GNNs) [35]–[37]. Since Large Language Models (LLMs) have recently shown powerful reasoning ability for textual data, researchers have attempted to adapt LLMs to understand graph-structured data [20]–[22]. However, existing research focuses on textual graphs where the information of nodes and edges can be transformed into text, thereby directly leveraging the textual reasoning ability of LLMs. These methods cannot be directly applied to our heterogeneous propagation graph of short-videos. To analyze the short-video propagation graph, where nodes can be texts, times, scalars, and videos, we propose a novel Large Graph Model (LGM) named NetGPT. NetGPT fuses open-source LLM (i.e., Qwen2-VL [18] in our experiments) and heterogeneous GNN to effectively comprehend and analyze the short-video propagation graph. Figure 6 illustrates the framework of our three-stage method.

4.1 Heterogeneous Graph Pretraining

Given the short-video propagation graph $G = \{V, E, S\}$ formulated in Section 3.6 and Tables 3–4, we first extract the raw features of all heterogenous nodes in V . For each node v of the video modality, we utilize the ViT [38] in Qwen2-VL-7B-Instruct⁴ to extract the video feature with an average pooling operation, as follows:

$$f^v = Avg\text{-Pooling}(ViT(v)) \in \mathbb{R}^{3584}, \quad (3)$$

where $Avg\text{-Pooling}(\cdot)$ is the average pooling operation that computes the average feature of the spatial-temporal features outputted by the ViT. For each node v of the text modality (including platforms, topics, titles, and descriptions), we utilize the RoBERTa [39], [40] of the Chinese-RoBERTa-wm-ext-large version⁵ to extract the text feature, as follows:

$$f^v = RoBERTa(v) \in \mathbb{R}^{1024}. \quad (4)$$

For each node v of the time modality (including times and ctimes), as v is formulated in the timestamp format, we

4. <https://huggingface.co/Qwen/Qwen2-VL-7B-Instruct>

5. <https://huggingface.co/hfl/chinese-roberta-wm-ext-large>

TABLE 3
Statistics of nodes in our constructed propagation graph of XS-Video.

Node				
Name	Description	Format	Example	Number
video	Visual content of a short-video	MP4	-	381,926
platform	Post platform of a short-video	Text	Douyin	5
topic	Topic keywords of a short-video	Text	Student, funeral, ask for leave, dormitory administrator...	535
title	Title of a short-video	Text	On January 25th, in Guangzhou, Guangdong, the school responded to the student to be blocked for leave. . .	381,926
description	Description of the video content	Text	A student was stopped from asking for leave in the early hours of the morning because of a funeral at home...	381,926
time	Post time of a short-video	Time	2024-11-25 21:18:52	381,926
ctime	Sampling time of a short-video sample	Time	2024-11-26	381,926
video_time	Duration of a short-video in seconds	Scalar	7	381,926
comment	Content of a comment of a short-video sample	Text+Time	Maximize embarrassment with the least amount of power... 2024-11-25 21:24:12	923,045
likes	Like number of a short-video sample	Scalar	2336	381,926
collects	Collection number of a short-video sample	Scalar	243	381,926
views	View number of a short-video sample	Scalar	12563	381,926
shares	Share number of a short-video sample	Scalar	260	381,926
comments	Comment number of a short-video sample	Scalar	645	381,926
fans	Fans number of the poster of a short-video sample	Scalar	26572246	381,926
All	Sum of above nodes	-	-	5,506,697

TABLE 4
Statistics of edges in our constructed propagation graph of XS-Video.

Edge				
Head Entity	Relation	Tail Entity	Description	Number
platform	is_platform_of	video	The platform of a short-video	381,926
topic	is_topic_of	video	The topic of a short-video	381,926
title	is_title_of	video	The title of a short-video	381,926
description	is_description_of	video	The description of a short-video	381,926
time	is_post_time_of	video	The post time of a short-video	381,926
ctime	is_current_time_of	video	The current time of a short-video sample	381,926
video_time	is_duration_time_of	video	The duration time of a short-video	381,926
comment	is_comment_of	video	A comment of a short-video sample	923,045
likes	is_likes_of	video	The like number of a short-video sample	381,926
collects	is_collects_of	video	The collection number of a short-video sample	381,926
views	is_views_of	video	The play/view number of a short-video sample	381,926
shares	is_shares_of	video	The share number of a short-video sample	381,926
comments	is_comments_of	video	The comment number of a short-video sample	381,926
fans	is_fans_of	video	The fans number of the poster of a short-video sample	381,926
video	has_same_author_as	video	The head (posted earlier) has the same author as the tail (posted later)	5,372,152
video	has_same_topic_as	video	The head (posted earlier) has the same topic as the tail (posted later)	1,655,971,954
video	is_history_of	video	The head (posted earlier) is the historical state of the tail (posted later)	484,364
-	-	-	Sum of above edges	1,667,716,553

utilize Sinusoidal Encoding [41] to compute the time feature, as follows:

$$\begin{aligned} f_{2i}^v &= \sin(v/10000^{2i/512}), i = 0, \dots, 255, \\ f_{2i+1}^v &= \cos(v/10000^{2i/512}), i = 0, \dots, 255, \end{aligned} \quad (5)$$

where $f^v \in \mathbb{R}^{512}$ can capture the relative time-spanning information. For each node v of the scalar value (including likes, collects, views, shares, comments, and fans), we directly use the logarithmic values as the raw feature, as follows:

$$f^v = \log(v + 1) \in \mathbb{R}^1. \quad (6)$$

Specially, each comment node contains the content text and the comment time, thereby we separately extract two features and concatenate them to the comment feature, as follows:

$$f^v = (f_{text}^v || f_{time}^v) \in \mathbb{R}^{1536}, \quad (7)$$

where $(\cdot || \cdot)$ is the vector concatenation operation, $f_{text}^v \in \mathbb{R}^{1024}$ is the text feature extracted by RoBERTa and $f_{time}^v \in$

\mathbb{R}^{512} is the time feature encoded by Sinusoidal Encoding. After obtaining the raw features $F = \{f_v | v \in V\}$ of all nodes, we compute the high-level features that capture both node information and edge structures by adopting heterogenous GNN, as follows:

$$F' = \{f'_v | v \in V\} = GNN(F_{raw}, E), \quad (8)$$

where $f'_v \in \mathbb{R}^{d_g}$ is the output feature of the node v , d_g is the dimension of the feature, and $GNN(\cdot, \cdot)$ is a 2-layer RGCN [42]. Then, we add a 1-layer predictor layer and pretrain the GNN with the predictor by Smooth L1 loss [43], as follows:

$$\begin{aligned} \hat{y}_v &= 9 \cdot \text{sigmoid}(\mathbf{W}_1 f'_v + b_1) \in (0, 9), \\ \mathcal{L}_{pt} &= \frac{1}{|S_{tra}|} \sum_{v \in S_{tra}} \text{SmoothL1}(\hat{y}_v, y_v), \end{aligned} \quad (9)$$

where $\mathbf{W}_1 \in \mathbb{R}^{1 \times d_g}$ and $b_1 \in \mathbb{R}$ are trained parameters of the predictor layer, y_v is the ground truth influence level, $\text{sigmoid}(\cdot)$ is the sigmoid function that scales output into

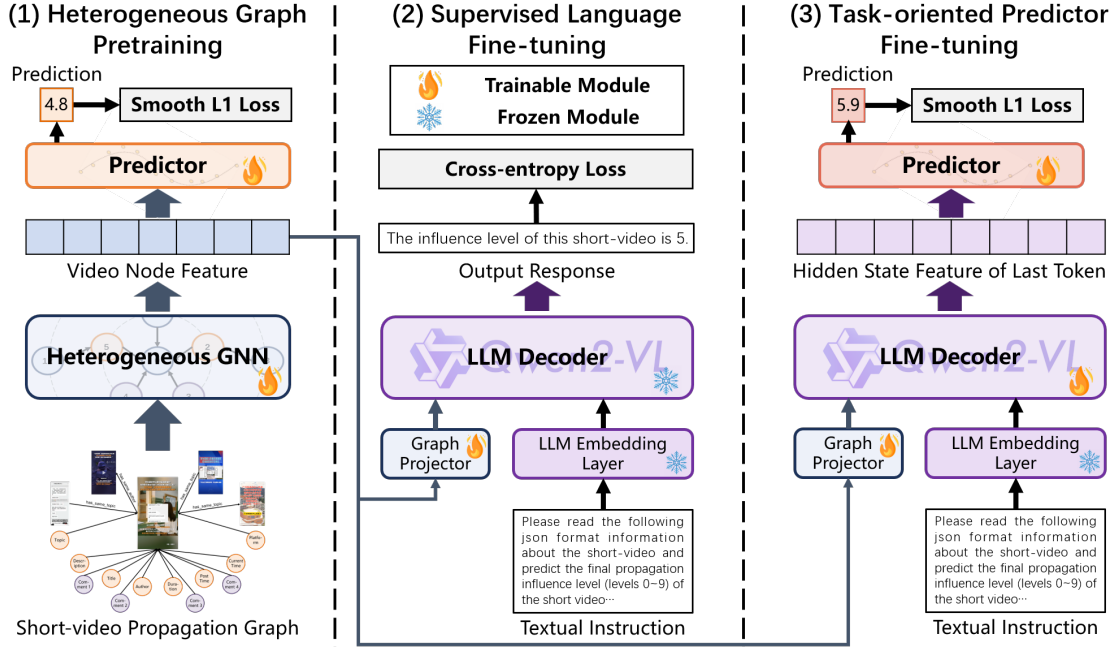


Fig. 6. Framework of our proposed NetGPT model: (1) Pretrain a heterogeneous GNN to obtain the features of the video nodes; (2) Train a graph projector to bridge GNN feature space and the LLM embedding space by supervised instruction fine-tuning; (3) Fine-tuning the model with an additional predictor to obtain the final influence level of the short-videos.

$(0, 1)$, S_{tra} is the set of all video nodes in the training set, and $SmoothL1(\cdot, \cdot)$ is the Smooth L1 loss. After optimizing the pretraining loss \mathcal{L}_{pt} , we obtain the heterogeneous graph encoder $GNN(\cdot, \cdot)$, which will be adopted in the following stages.

4.2 Supervised Language Fine-tuning

Given the pretrained graph encoder $GNN(\cdot, \cdot)$ and an open-source LLM $LLM(\cdot)$ (e.g., Qwen2-VL in our experiments), this stage aims to align the graph feature space of GNN and the token embedding space of LLM. Frozen the pretrained GNN, we utilize a linear projector to transform f'_v into the token embedding space, as follows:

$$e_v = \mathbf{W}_2 f'_v + b_2, \quad (10)$$

where $\mathbf{W}_2 \in \mathbb{R}^{d_{lm} \times d_g}$ and $b_2 \in \mathbb{R}^{d_{lm}}$ are trainable parameters, and d_{lm} is the token embedding dimension of the LLM. Next, we construct the input instruction ins for LLM, which is “You are a helpful assistant. Graph: (v, E) . Please read the following json format information about the short-video and predict the final propagation influence level (levels 0-9) of the short video: x_v ”, where x_v is the textual information of the sample (as shown in Figure 2 except the influence level) in the json format. More details of our instruction are introduced in Appendix 4.3. Then, we obtain the input token embeddings of ins , where the embedding of (v, E) is e_v computed by Equations 8 and 10, and the embeddings of other textual tokens are obtained by the embedding layer of the LLM. The ground truth output of this stage is constructed as response $res = \text{“The influence level of this short-video is } y_v\text{”}$, where y_v is the ground truth influence level of v . The optimization objective of this stage is maximizing the generation probability of res with the input ins , as follows:

$$\max P_{LLM}(res|ins), \quad (11)$$

where $P_{LLM}(\cdot|\cdot)$ is the generation probability function of the LLM. Following the original implementation of Qwen2-VL [18], we leverage the cross-entropy loss to optimize the Equation 11. Specially, to preserve the pretrained knowledge and avoid the model corruption introduced by fusing GNN and LLM, we only train the parameters \mathbf{W}_2 and b_2 of the graph feature projector, while keeping all parameters of the pretrained GNN and LLM frozen.

4.3 Prompt Instruction for Fine-tuning

In supervised language fine-tuning and the following task-oriented predictor fine-tuning, we combine the graph feature and the textual information for SPIR. Assume x_v is the textual information of the video v in the json format, the detailed input prompt is as follows:

```

< |im_start| > system
You are a helpful assistant. < |im_end| >
< |im_start| > user
Graph 1 : < |graph_start| > < |graph_pad| >
< |graph_end| > Please read the following json format
information about the short-video and predict the final
propagation influence level (levels 0-9) of the short-video :
x_v < |im_end| >
< |im_start| > assistant
  
```

where $\langle |im_start| \rangle$ and $\langle |im_end| \rangle$ are start-of-message and end-of-message tokens of Qwen2-VL. Specially, we add $\langle |graph_start| \rangle$, $\langle |graph_pad| \rangle$, and $\langle |graph_end| \rangle$ tokens into the vocabulary, where $\langle |graph_start| \rangle$ and $\langle |graph_end| \rangle$ are start-of-graph and end-of-graph tokens trainable during the last two training stages. $\langle |graph_pad| \rangle$ is a placeholder and its

```

<|im_start|>system
You are a helpful assistant.<|im_end|>
<|im_start|>user
Graph 1: <|graph_start|><|graph_pad|><|graph_end|>Please read
the following json format information about the short-video and
predict the final propagation influence level (levels 0~9) of the short-
video: {"description": "A student was stopped from asking for leave in
the early hours of the morning because of a funeral at home. He
knelt down before the dormitory administrator and was not allowed
to leave. She did not see her loved one for the last time...", "title": "On
January 25th, in Guangzhou, Guangdong, the school responded to
the student to be blocked for leave...", "post user ID":
"2638453861807501", "video duration (s)": 7, "platform": "douyin",
"post time": "2024-11-25 21:18:52", "topic": "Student, funeral, ask for
leave, dormitory administrator, not allowed", "current time": "2024-
11-26", "current fans": 26572246, "current likes": 2336, "current views":
null, "current shares": 260, "current collects": 243, "current comments":
645, "comment list": {"0": {"comment content": "Must be
fired.", "comment time": "2024-11-25 21:26:47"}, "1": {"comment
content": "Who is lying?","comment time": "2024-11-25
21:48:16"}, "2": {"comment content": "power","comment time":
"2024-11-25 21:28:58"}, "3": {"comment content": "classic
rhetoric","comment time": "2024-11-25 22:04:25"}, "4": {"comment
content": "XX","comment time": "2024-11-25 21:52:14"}, "5":
{"comment content": "Maximize embarrassment with the least
amount of power[smile].","comment time": "2024-11-25 21:24:12"}}}
<|im_end|>
<|im_start|>assistant

```

Fig. 7. An example of the input instruction in our method. The text is translated into English.

embedding will be replaced by the graph embedding e_v in Equation 10. We show an example of the input instruction in Figure 7

4.4 Task-oriented Predictor Fine-tuning

After training the graph feature projector, the LLM can comprehend the node v in the graph G . This stage aims further to improve the ability of the LLM for SPIR. Since the LLM constructs the attention correlations between the last token and all tokens in ins , we leverage the output hidden state feature f_h of the last token. We add a task-oriented regression predictor to forecast the influence level, as follows:

$$\tilde{y}_v = 9 \cdot \text{sigmoid}(\mathbf{W}_3 f_h + b_3) \in (0, 9), \quad (13)$$

where $\mathbf{W}_3 \in \mathbb{R}^{1 \times d_{im}}$ and $b_3 \in \mathbb{R}$ are trainable parameters of the predictor. Finally, we compute the Smooth L1 loss to train the predictor, the LLM, and the graph feature projector jointly, as follows:

$$\mathcal{L}_{ft} = \frac{1}{|S_{tra}|} \sum_{v \in S_{tra}} \text{SmoothL1}(\tilde{y}_v, y_v), \quad (14)$$

where S_{tra} is the set of all video nodes in the training set and $\text{SmoothL1}(\cdot, \cdot)$ is the Smooth L1 loss.

5 EXPERIMENTS

5.1 Experimental Setup

Baseline methods. We adopt 10 state-of-the-art baseline methods, including 4 GNNs, 4 LLMs, and 2 multimodal LLMs. The adopted 4 GNN baselines are GCN [44], HAN

[45], HetSANN [35], and RGCN [46]. The adopted 4 LLM baselines are Mistral-7B-Instruct-v0.3 [47], InternLM2.5-7B [48], Llama-3.1-8B-Instruct [49], and Qwen2.5-7B-Instruct [50]. We further adopt 2 multimodal LLM baselines that can comprehend the video modality, i.e., Llava-Next-Video-7B [19] and Qwen2-VL-7B-Instruct [18]. To conduct a fair comparison, we use the same input graph, predictor module, and optimization loss introduced in Section 4.1 for all GNN baselines. For LLM and multimodal LLM baselines, we use the same input instructions, output response, and optimization loss introduced in Section 4.2, where the information of the short-video is organized in the json format. Additionally, we input the video data into multimodal LLM baselines.

Implementation details. We adopt a 2-layer RGCN as the graph encoder and Qwen2-VL-7B-Instruct as the LLM backbone in our model. We utilize the DeepSpeed [51] framework and ZeRO-2 optimizer [52] to train our model on 8 Nvidia A800 80G GPUs. d_g is set to 1024. To improve robustness to varying lengths of the input samples while constructing the input instruction, we randomly select 50 comments of a sample if it has more than 50 comments. Moreover, we set the maximum number of tokens as 4000 when tokenizing the input instructions. In task-oriented predictor fine-tuning, we only train the last 4 layers of the LLM decoder while keeping other decoder layers frozen.

For all GNN baselines, we set the dimensionality of hidden and output features as the same as $d_g (= 1024)$ in our RGCN encoder. The number of layers is set to 2 which is also adopted in our GNN encoder. The minimum sampling number of neighborhood nodes is tuned and set as 50.

For all LLM and multimodal LLM baselines, we apply the same truncation strategy of inputs in our model. We utilize the LoRA algorithm [53] to efficiently optimize these models.

5.2 Metrics

Since we annotate the propagation influence of short-videos into the 0 to 9 levels, SPIR can be considered as a 10-class classification task. However, as the 0 to 9 levels represent a progressive increase in propagation influence, an inaccurate prediction closer to the ground truth is preferable to a prediction that differs significantly. Therefore, SPIR also exhibits traits of a regression task. To effectively evaluate the predicted results for SPIR, we adopt both widely-used metrics for classification and regression. Denote the ground truth for test samples as $\{y_i \in [10]\}_{i=1}^M$ and the predicted levels as $\{\tilde{y}_i\}_{i=1}^M$, where y_i is the label of the i -th test sample, \tilde{y}_i is the prediction of the i -th test sample, and M is the number of test samples. We calculate three metrics to evaluate the prediction.

Accuracy (ACC). Following widely-used evaluation for the classification task [54]–[56], we compute the Accuracy (ACC) of the predicted results as follows:

$$ACC = P(y_i = \text{rounding}(\tilde{y}_i)), i \in [M], \quad (15)$$

where $\text{rounding}(\cdot)$ is the rounding function.

Mean Squared Error (MSE). Following widely-used evaluation for the regression task [1], [55], [57], we compute the Mean Squared Error (MSE) of the predicted results as follows:

$$MSE = E_{i \in [M]} \{(y_i - \tilde{y}_i)^2\}. \quad (16)$$

TABLE 5

The results of Short-video Propagation Influence Rating (SPIR) on the XS-Video dataset. \uparrow denotes the higher the better and \downarrow denotes the lower the better.

Model	Input	ACC \uparrow	MSE \downarrow	MAE \downarrow
GCN	Graph	0.4474	1.0623	0.7599
HAN	Graph	0.2619	2.6666	1.2724
HetSANN	Graph	0.5078	0.8917	0.6803
RGCN	Graph	0.6313	0.7801	0.5844
Mistral-v0.3	Text	0.5387	2.1000	0.8123
InternLM2.5	Text	0.5268	2.1110	0.8064
Llama-3.1	Text	0.5290	2.1215	0.8081
Qwen2.5	Text	0.5469	2.0820	0.7688
Llava-Next-Video	Text+Video	0.5694	1.8503	0.7315
Qwen2-VL	Text+Video	0.5884	1.6820	0.6629
NetGPT (Ours)	Graph+Text	0.6777	0.7169	0.5457

Mean Absolute Error (MAE). Moreover, we compute the Mean Absolute Error (MAE) for regression of the predicted results as follows:

$$MAE = E_{i \in [M]} \{|y_i - \bar{y}_i|\}. \quad (17)$$

We note that ACC is the higher the better while MSE and MAE are the lower the better.

5.3 Results and Discussions

The experimental results on our XS-Video dataset are shown in Table 5. From the results, we have the following observations:

- Small GNN models (i.e., GCN, HAN, HetSANN, and RGCN) perform worse than our large graph model (i.e., NetGPT). Compared to the best small GNN (RGCN), our NetGPT relatively increases ACC by 7.3% and decreases MSE and MAE by 8.1% and 6.6%. These results show that bridging graph-structured data with LLM and leveraging large-scale pretrained knowledge can significantly improve SPIR.
- The performance of methods without inputting the propagation graph (i.e., LLMs and multimodal LLMs) is suboptimal compared to RGCN and our NetGPT. Our NetGPT relatively outperforms the best multimodal LLM (Qwen2-VL) by 15.2%(\uparrow), 57.4%(\downarrow), and 17.7%(\downarrow) in terms of ACC, MSE, and MAE, respectively. These results show that capturing the propagation relations in the short-video propagation graph is essential for performing our proposed SPIR task.
- RGCN performs much better than GCN, which further captures the heterogeneity of nodes and edges in the propagation graph. This shows that graph heterogeneity is an important factor in the SPIR task. Moreover, multimodal LLMs with both text and video input outperform LLMs, which shows the content and quality of the videos are also important in SPIR.

5.4 Ablation Study

We design several variants of our NetGPT to conduct the ablation study, as follows: **NetGPT-V** replaces the raw video features in Equation 3 by zero vectors; **NetGPT-VV** deletes all edges among video nodes in the propagation graph; **NetGPT-IV** deletes all edges from the interactive information nodes (i.e., ctimes, fans, likes, comments, shares,

TABLE 6

Ablation results on the XS-Video test set.

Model	ACC	MSE	MAE
NetGPT-V	0.6564	0.7415	0.5669
NetGPT-VV	0.5889	0.8935	0.6386
NetGPT-IV	0.2805	2.2839	1.1688
NetGPT-CV	0.6464	0.8249	0.5868
NetGPT-SLF	0.6552	0.7366	0.5605
NetGPT-2B	0.6695	0.7307	0.5563
NetGPT (Ours)	0.6777	0.7169	0.5457

views, collects) to the video nodes; **NetGPT-CV** deletes all edges from the comment content nodes to the video nodes; **NetGPT-SLF** abandons the supervised language fine-tuning introduced in Section 4.2 in our method; **NetGPT-2B** replaces the backbone LLM Qwen2-VL-7B-Instruct by Qwen2-VL-2B-Instruct.

As shown in Table 6, we have the following observations: (1) NetGPT-V performs worse than NetGPT, which shows the importance of considering the video content information. (2) NetGPT-VV, NetGPT-IV, and NetGPT-CV perform worse than NetGPT, which shows the edges from video nodes, interactive information nodes, and comment content nodes to video nodes are significant. (3) NetGPT-SLF underperforms NetGPT, which verifies the effectiveness of our three-stage training mechanism. (4) With a smaller LLM backbone, NetGPT-2B performs worse than NetGPT, which indicates the effectiveness of leveraging pretrained knowledge of larger LLMs.

5.5 Results of Short- and Long-term Prediction

To further analyze the prediction of different periods, we compute the MSE and MAE of test samples with the observation periods (i.e., current time – post time) of ≤ 3 days, ≤ 7 days, and > 7 days. We demonstrate the box diagrams in Figure 8 and compare the results of our NetGPT with the best baseline RGCN. From the results, we have the following observations: (1) For all observation periods, our NetGPT outperforms RGCN in terms of median and average of MSE and MAE. These results further demonstrate the superiority of our method. (2) For all observation periods, our NetGPT outperforms RGCN in terms of first quartile, third quartile, and maximum of MSE and MAE. These results further demonstrate the better prediction robustness of our method. (3) For both methods, when the observation period increases, the MSE and MAE of the finally achieved propagation influence levels significantly decrease. These results show the difficulty of our proposed dataset and task that the long-term prediction performance needs improvements.

5.6 Convergence on Different Platforms

Short-video platforms can differ in sample numbers and propagation patterns. In this section, we analyze the model convergence on different platforms. In Figure 9, we show the ACC and MSE of training samples from different platforms during the 200th-4000th optimization steps in the task-oriented predictor fine-tuning procedure. (1) The ACC and MSE of Bilibili, which has the fewest samples, quickly converge during fine-tuning, showing the potential over-fitting problem of this small platform. (3) Interestingly, the ACC

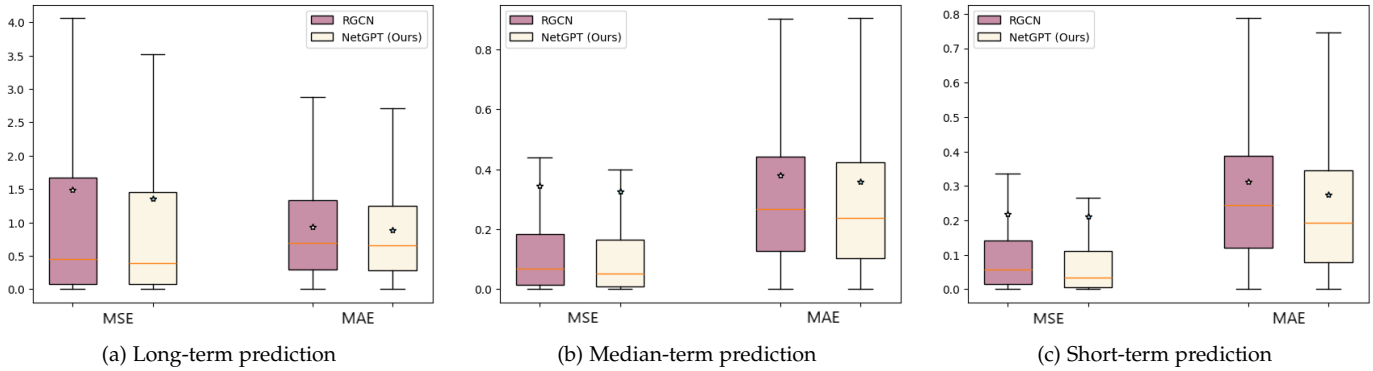


Fig. 8. Results of long-, median-, and short-term prediction with the observation times of ≤ 3 days, ≤ 7 days, and > 7 days.

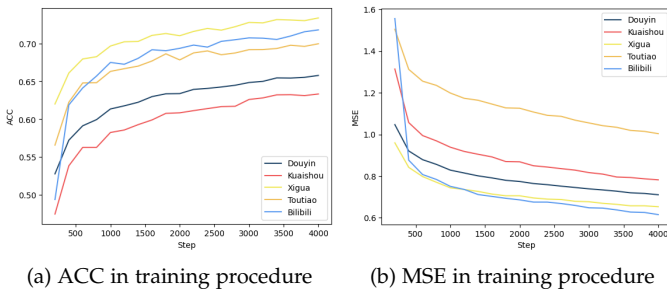


Fig. 9. Training procedure on our XS-Video dataset.

and MSE of Xigua, the second largest platform, also converge quickly, which shows that the propagation patterns on Xigua may be relatively easy to recognize. (3) Overall, 5 platforms exhibit different convergence curves during the training procedure, which indicates the fundamental difference in propagation on these platforms. Therefore, our proposed XS-Video dataset collects data from these 5 biggest Chinese platforms to facilitate a more comprehensive analysis of short-video propagation.

6 DISCUSSION AND CONCLUSION

In this paper, we propose a Cross-platform Short-Video (XS-Video) dataset with 381,926 samples from the 5 biggest Chinese platforms, including short-video content, post information, interactive information, comment content, and elaborately annotated propagation levels, for short-video propagation analysis. Based on our dataset, we propose a new Short-video Propagation Influence Rating (SPIR) task, which aims to predict the long-term propagation influence of a newly posted short-video, under the background of a huge propagation network. Moreover, utilizing the entities and relations present in XS-Video, we construct a huge propagation graph consisting of 5.5 million nodes and 1.7 billion directed edges. We build a comprehensive benchmark for SPIR by evaluating state-of-the-art methods, including GNNs, LLMs, and multimodal LLMs. To perform SPIR, we propose NetGPT, a novel large graph model to bridge heterogeneous graph data and LLMs. Extensive experiments demonstrate that NetGPT significantly outperforms state-of-the-art methods for SPIR.

REFERENCES

- [1] S. Tang, Q. Li, X. Ma, C. Gao, D. Wang, Y. Jiang, Q. Ma, A. Zhang, and H. Chen, "Knowledge-based temporal fusion network for interpretable online video popularity prediction," in *Proceedings of the ACM Web Conference 2022*, 2022, pp. 2879–2887.
- [2] T. Zhong, J. Lang, Y. Zhang, Z. Cheng, K. Zhang, and F. Zhou, "Predicting micro-video popularity via multi-modal retrieval augmentation," in *Proceedings of the 47th International ACM SIGIR Conference on Research and Development in Information Retrieval*, 2024, pp. 2579–2583.
- [3] J. Song and J. Liu, "A data-driven short video international communication model based on indicator system communication network and attention bilstm neural network," *Scientific Reports*, vol. 14, no. 1, p. 14532, 2024.
- [4] J. Chen, X. Song, L. Nie, X. Wang, H. Zhang, and T.-S. Chua, "Micro tells macro: Predicting the popularity of micro-videos via a transductive model," in *Proceedings of the 24th ACM international conference on Multimedia*, 2016, pp. 898–907.
- [5] J. Xie, Y. Zhu, Z. Zhang, J. Peng, J. Yi, Y. Hu, H. Liu, and Z. Chen, "A multimodal variational encoder-decoder framework for micro-video popularity prediction," in *Proceedings of the web conference 2020*, 2020, pp. 2542–2548.
- [6] J. Xie, Y. Zhu, and Z. Chen, "Micro-video popularity prediction via multimodal variational information bottleneck," *IEEE Transactions on Multimedia*, vol. 25, pp. 24–37, 2021.
- [7] M. Cha, H. Kwak, P. Rodriguez, Y.-Y. Ahn, and S. Moon, "Analyzing the video popularity characteristics of large-scale user generated content systems," *IEEE/ACM Transactions on networking*, vol. 17, no. 5, pp. 1357–1370, 2009.
- [8] Y. Borghol, S. Ardon, N. Carlsson, D. Eager, and A. Mahanti, "The untold story of the clones: Content-agnostic factors that impact youtube video popularity," in *Proceedings of the 18th ACM SIGKDD international conference on Knowledge discovery and data mining*, 2012, pp. 1186–1194.
- [9] L. Yuan, H. Xia, and Q. Ye, "The effect of advertising strategies on a short video platform: evidence from tiktok," *Industrial Management & Data Systems*, vol. 122, no. 8, pp. 1956–1974, 2022.
- [10] L. Xiao, X. Li, and Y. Zhang, "Exploring the factors influencing consumer engagement behavior regarding short-form video advertising: A big data perspective," *Journal of Retailing and Consumer Services*, vol. 70, p. 103170, 2023.
- [11] Q. Cai, Z. Xue, C. Zhang, W. Xue, S. Liu, R. Zhan, X. Wang, T. Zuo, W. Xie, D. Zheng *et al.*, "Two-stage constrained actor-critic for short video recommendation," in *Proceedings of the ACM Web Conference 2023*, 2023, pp. 865–875.
- [12] S. Zhang, Z. He, Z. Ye, P. Sun, Q. Ai, M. Zhang, and Y. Liu, "Eeg-svrec: An eeg dataset with user multidimensional affective engagement labels in short video recommendation," in *Proceedings of the 47th International ACM SIGIR Conference on Research and Development in Information Retrieval*, 2024, pp. 698–708.
- [13] X. Chen, D. B. Valdovinos Kaye, and J. Zeng, "# positiveenergy douyin: Constructing "playful patriotism" in a chinese short-video application," *Chinese Journal of Communication*, vol. 14, no. 1, pp. 97–117, 2021.
- [14] J. Qin, Q. Du, Y. Deng, B. Zhang, and X. Sun, "How does short video use generate political identity? intermediate mechanisms

- with evidence from china's small-town youth," *Frontiers in Psychology*, vol. 14, p. 1107273, 2023.
- [15] A. Liu, B. Feng, B. Xue, B. Wang, B. Wu, C. Lu, C. Zhao, C. Deng, C. Zhang, C. Ruan *et al.*, "Deepseek-v3 technical report," *arXiv preprint arXiv:2412.19437*, 2024.
- [16] C. Wu, X. Chen, Z. Wu, Y. Ma, X. Liu, Z. Pan, W. Liu, Z. Xie, X. Yu, C. Ruan *et al.*, "Janus: Decoupling visual encoding for unified multimodal understanding and generation," *arXiv preprint arXiv:2410.13848*, 2024.
- [17] D. Xue, S. Qian, and C. Xu, "Few-shot multimodal explanation for visual question answering," in *Proceedings of the 32nd ACM International Conference on Multimedia*, 2024, pp. 1875–1884.
- [18] P. Wang, S. Bai, S. Tan, S. Wang, Z. Fan, J. Bai, K. Chen, X. Liu, J. Wang, W. Ge *et al.*, "Qwen2-vl: Enhancing vision-language model's perception of the world at any resolution," *arXiv preprint arXiv:2409.12191*, 2024.
- [19] F. Li, R. Zhang, H. Zhang, Y. Zhang, B. Li, W. Li, Z. Ma, and C. Li, "Llava-next-interleave: Tackling multi-image, video, and 3d in large multimodal models," *arXiv preprint arXiv:2407.07895*, 2024.
- [20] J. Tang, Y. Yang, W. Wei, L. Shi, L. Su, S. Cheng, D. Yin, and C. Huang, "Graphgpt: Graph instruction tuning for large language models," in *Proceedings of the 47th International ACM SIGIR Conference on Research and Development in Information Retrieval*, 2024, pp. 491–500.
- [21] J. Li, X. Sun, Y. Li, Z. Li, H. Cheng, and J. X. Yu, "Graph intelligence with large language models and prompt learning," in *Proceedings of the 30th ACM SIGKDD Conference on Knowledge Discovery and Data Mining*, 2024, pp. 6545–6554.
- [22] H. Wang, S. Feng, T. He, Z. Tan, X. Han, and Y. Tsvetkov, "Can language models solve graph problems in natural language?" *Advances in Neural Information Processing Systems*, vol. 36, 2024.
- [23] S. D. Roy, T. Mei, W. Zeng, and S. Li, "Towards cross-domain learning for social video popularity prediction," *IEEE Transactions on multimedia*, vol. 15, no. 6, pp. 1255–1267, 2013.
- [24] J. Chen, "Multi-modal learning: Study on a large-scale micro-video data collection," in *Proceedings of the 24th ACM international conference on Multimedia*, 2016, pp. 1454–1458.
- [25] P. Jing, Y. Su, L. Nie, X. Bai, J. Liu, and M. Wang, "Low-rank multi-view embedding learning for micro-video popularity prediction," *IEEE Transactions on Knowledge and Data Engineering*, vol. 30, no. 8, pp. 1519–1532, 2017.
- [26] L. Tang, Q. Huang, A. Puntambekar, Y. Vigfusson, W. Lloyd, and K. Li, "Popularity prediction of facebook videos for higher quality streaming," in *2017 USENIX Annual Technical Conference (USENIX ATC 17)*, 2017, pp. 111–123.
- [27] N. Ou, L. Yu, H. Li, Q. Du, J. Xiang, and W. Gong, "Mtaf: Shopping guide micro-videos popularity prediction using multimodal and temporal attention fusion approach," in *ICASSP 2022-2022 IEEE International Conference on Acoustics, Speech and Signal Processing (ICASSP)*. IEEE, 2022, pp. 4543–4547.
- [28] W. Hu, Y. Xu, Y. Li, W. Li, Z. Chen, and Z. Tu, "Bliva: A simple multimodal llm for better handling of text-rich visual questions," in *Proceedings of the AAAI Conference on Artificial Intelligence*, vol. 38, no. 3, 2024, pp. 2256–2264.
- [29] Z. Ge, H. Huang, M. Zhou, J. Li, G. Wang, S. Tang, and Y. Zhuang, "Worldgpt: Empowering llm as multimodal world model," in *Proceedings of the 32nd ACM International Conference on Multimedia*, 2024, pp. 7346–7355.
- [30] J. Cha, W. Kang, J. Mun, and B. Roh, "Honeybee: Locality-enhanced projector for multimodal llm," in *Proceedings of the IEEE/CVF Conference on Computer Vision and Pattern Recognition*, 2024, pp. 13817–13827.
- [31] J. Li, X. Wang, S. Zhu, C.-W. Kuo, L. Xu, F. Chen, J. Jain, H. Shi, and L. Wen, "Cumio: Scaling multimodal llm with co-upcycled mixture-of-experts," *Advances in Neural Information Processing Systems*, vol. 37, pp. 131224–131246, 2025.
- [32] A. M. Rashid, G. Karypis, and J. Riedl, "Influence in ratings-based recommender systems: An algorithm-independent approach," in *Proceedings of the 2005 SIAM International Conference on Data Mining*. SIAM, 2005, pp. 556–560.
- [33] P. Cui, F. Wang, S. Liu, M. Ou, S. Yang, and L. Sun, "Who should share what? item-level social influence prediction for users and posts ranking," in *Proceedings of the 34th international ACM SIGIR conference on Research and development in Information Retrieval*, 2011, pp. 185–194.
- [34] Y. Liu, X. Cao, and Y. Yu, "Are you influenced by others when rating? improve rating prediction by conformity modeling," in *Proceedings of the 10th ACM conference on recommender systems*, 2016, pp. 269–272.
- [35] H. Hong, H. Guo, Y. Lin, X. Yang, Z. Li, and J. Ye, "An attention-based graph neural network for heterogeneous structural learning," in *Proceedings of the AAAI conference on artificial intelligence*, vol. 34, no. 04, 2020, pp. 4132–4139.
- [36] S. B. Yussif, N. Xie, Y. Yang, and H. T. Shen, "Self-relational graph convolution network for skeleton-based action recognition," in *Proceedings of the 31st ACM International Conference on Multimedia*, 2023, pp. 27–36.
- [37] J. Hu, B. Hooi, and B. He, "Efficient heterogeneous graph learning via random projection," *IEEE Transactions on Knowledge and Data Engineering*, 2024.
- [38] A. Dosovitskiy, "An image is worth 16x16 words: Transformers for image recognition at scale," *arXiv preprint arXiv:2010.11929*, 2020.
- [39] Y. Liu, M. Ott, N. Goyal, J. Du, M. Joshi, D. Chen, O. Levy, M. Lewis, L. Zettlemoyer, and V. Stoyanov, "Roberta: A robustly optimized bert pretraining approach," *ArXiv*, vol. abs/1907.11692, 2019. [Online]. Available: <https://api.semanticscholar.org/CorpusID:198953378>
- [40] Y. Cui, W. Che, T. Liu, B. Qin, and Z. Yang, "Pre-training with whole word masking for chinese bert," *IEEE/ACM Transactions on Audio, Speech, and Language Processing*, vol. 29, pp. 3504–3514, 2021.
- [41] A. Vaswani, N. Shazeer, N. Parmar, J. Uszkoreit, L. Jones, A. N. Gomez, L. u. Kaiser, and I. Polosukhin, "Attention is all you need," in *Advances in Neural Information Processing Systems*, vol. 30. Curran Associates, Inc., 2017.
- [42] M. Schlichtkrull, T. N. Kipf, P. Bloem, R. Van Den Berg, I. Titov, and M. Welling, "Modeling relational data with graph convolutional networks," in *The semantic web: 15th international conference, ESWC 2018, Heraklion, Crete, Greece, June 3–7, 2018, proceedings 15*. Springer, 2018, pp. 593–607.
- [43] R. Girshick, "Fast r-cnn," 2015.
- [44] T. N. Kipf and M. Welling, "Semi-supervised classification with graph convolutional networks," in *International Conference on Learning Representations (ICLR)*, 2017.
- [45] X. Wang, H. Ji, C. Shi, B. Wang, Y. Ye, P. Cui, and P. S. Yu, "Heterogeneous graph attention network," in *The world wide web conference*, 2019, pp. 2022–2032.
- [46] M. Zhang, H. Liu, C. Chen, G. Gao, H. Li, and J. Zhao, "Access-fixer: Enhancing gui accessibility for low vision users with r-gen model," *IEEE Transactions on Software Engineering*, vol. 50, no. 2, pp. 173–189, 2024.
- [47] A. Q. Jiang, A. Sablayrolles, A. Mensch, C. Bamford, D. S. Chaplot, D. d. l. Casas, F. Bressand, G. Lengyel, G. Lample, L. Saulnier *et al.*, "Mistral 7b," *arXiv preprint arXiv:2310.06825*, 2023.
- [48] Z. Cai, M. Cao, H. Chen, K. Chen, K. Chen, X. Chen, X. Chen, Z. Chen, Z. Chen, P. Chu, X. Dong, H. Duan, Q. Fan, Z. Fei, Y. Gao, J. Ge, C. Gu, Y. Gu, T. Gui, A. Guo, Q. Guo, C. He, Y. Hu, T. Huang, T. Jiang, P. Jiao, Z. Jin, Z. Lei, J. Li, J. Li, L. Li, S. Li, W. Li, Y. Li, H. Liu, J. Liu, J. Hong, K. Liu, X. Liu, C. Lv, H. Lv, K. Lv, L. Ma, R. Ma, Z. Ma, W. Ning, L. Ouyang, J. Qiu, Y. Qu, F. Shang, Y. Shao, D. Song, Z. Song, Z. Sui, P. Sun, Y. Sun, H. Tang, B. Wang, G. Wang, J. Wang, J. Wang, R. Wang, Y. Wang, Z. Wang, X. Wei, Q. Weng, F. Wu, Y. Xiong, C. Xu, R. Xu, H. Yan, Y. Yan, X. Yang, H. Ye, H. Ying, J. Yu, J. Yu, Y. Zang, C. Zhang, L. Zhang, P. Zhang, P. Zhang, R. Zhang, S. Zhang, S. Zhang, W. Zhang, W. Zhang, X. Zhang, X. Zhang, H. Zhao, Q. Zhao, X. Zhao, F. Zhou, Z. Zhou, J. Zhuo, Y. Zou, X. Qiu, Y. Qiao, and D. Lin, "Internlm2 technical report," 2024.
- [49] A. Dubey, A. Jauhri, A. Pandey, A. Kadian, A. Al-Dahle, A. Letman, A. Mathur, A. Schelten, A. Yang, A. Fan *et al.*, "The llama 3 herd of models," *arXiv preprint arXiv:2407.21783*, 2024.
- [50] A. Yang, B. Yang, B. Zhang, B. Hui, B. Zheng, B. Yu, C. Li, D. Liu, F. Huang, H. Wei *et al.*, "Qwen2. 5 technical report," *arXiv preprint arXiv:2412.15115*, 2024.
- [51] J. Rasley, S. Rajbhandari, O. Ruwase, and Y. He, "Deepspeed: System optimizations enable training deep learning models with over 100 billion parameters," in *Proceedings of the 26th ACM SIGKDD International Conference on Knowledge Discovery & Data Mining*, 2020, pp. 3505–3506.
- [52] S. Rajbhandari, J. Rasley, O. Ruwase, and Y. He, "Zero: Memory optimizations toward training trillion parameter models," in *SC20: International Conference for High Performance Computing, Networking, Storage and Analysis*. IEEE, 2020, pp. 1–16.
- [53] E. J. Hu, Y. Shen, P. Wallis, Z. Allen-Zhu, Y. Li, S. Wang, L. Wang,

- W. Chen *et al.*, "Lora: Low-rank adaptation of large language models." *ICLR*, vol. 1, no. 2, p. 3, 2022.
- [54] R. M. Haralick, K. Shanmugam, and I. H. Dinstein, "Textural features for image classification," *IEEE Transactions on systems, man, and cybernetics*, no. 6, pp. 610–621, 1973.
- [55] A. Krizhevsky, I. Sutskever, and G. E. Hinton, "Imagenet classification with deep convolutional neural networks," *Advances in neural information processing systems*, vol. 25, 2012.
- [56] S. Qian, H. Chen, D. Xue, Q. Fang, and C. Xu, "Open-world social event classification," in *Proceedings of the ACM Web Conference 2023*, 2023, pp. 1562–1571.
- [57] N. Draper, *Applied regression analysis*. McGraw-Hill. Inc, 1998.